Oncogene (2004) 23, 1549–1557

www.nature.com/onc

Loss of CCAAT/enhancer binding protein δ promotes chromosomal instability

A-Mei Huang[1], Cristina Montagna[2], Shikha Sharan[1], Yajun Ni[1,3], Thomas Ried[2] and Esta Sterneck*[,1]

[1]*Regulation of Cell Growth Laboratory, PO Box B, Frederick, MD 21702, USA;* [2]*Genetics Branch, Center for Cancer Research, National Cancer Institute, NIH, 50 South Drive, Bethesda, MD 20892, USA*

The transcription factor CCAAT/enhancer binding protein δ (Cebpd, also known as C/EBPδ, CRP3, CELF, NF-IL6β) is implicated in diverse cellular functions such as the acute phase response, adipocyte differentiation, learning and memory, and mammary epithelial cell growth control. Here, we report that lack of Cebpd causes genomic instability and centrosome amplifications in primary embryonic fibroblasts derived from 129S1 mice. Upon spontaneous immortalization, Cebpd-deficient fibroblasts acquire transformed features such as impaired contact inhibition and reduced serum dependence. These data identify a novel role for Cebpd in the maintenance of chromosomal stability and suggest a potential tumor suppressor function *in vivo*.
Oncogene (2004) **23,** 1549–1557. doi:10.1038/sj.onc.1207285
Published online 12 January 2004

Keywords: C/EBP; tumor suppressor; mouse embryo fibroblast; chromosomal rearrangements; genomic instability

Introduction

The C/EBP family of transcription factors is comprised of five proteins: Cebpa, Cebpb, Cebpg, Cebpd, Cebpe (see mouse genome nomenclature: http://www.informatics.jax.org/mgihome/nomen/). Collectively, they are expressed in almost every cell type and a large body of data exists on their expression patterns, the promoters they regulate and the signals that modulate expression and/or activity. The great majority of this information was obtained *in vitro*. However, in recent years, mice have been generated with null mutations for each of the *Cebp* genes, allowing the identification of unique and physiologically relevant functions. This approach has demonstrated that individual *Cebp* genes can regulate the lineage commitment, growth or differentiation of specific cell types such as for example adipocytes and hepatocytes (*Cebpa*); ovarian granulosa cells, mammary epithelial cells and keratinocytes (*Cebpb*); and granulocytes (*Cebpe*) (Ramji and Foka, 2002).

Cebpd was first characterized as an acute phase inflammatory response gene. Expression is low to undetectable in most cell types and tissues. However, it is rapidly induced by a variety of extracellular stimuli, for example, growth hormone, insulin, IFNγ, IL-1, IL-6, LPS, TNFα, dexamethasone, noradrenalin and glutamate (Takiguchi, 1998; Ramji and Foka, 2002). In osteoblasts, Cebpd activity is associated with proliferation reponses (Umayahara *et al*., 1997; Billiard *et al*., 2001). In lung epithelial cells, Cebpd expression and activity are related to differentiation (Breed *et al*., 1997; Sugahara *et al*., 1999; Cassel *et al*., 2000). In the mouse mammary gland, Cebpd is highly expressed exclusively at the onset of involution, the period of postlactational mammary gland regression and tissue remodeling (Gigliotti and DeWille, 1998; Gigliotti and DeWille, 1999). Results from overexpression of either Cebpd or antisense Cebpd in a mouse mammary epithelial cell line suggest that Cebpd promotes growth arrest in this cell type (O'Rourke *et al*., 1999). In fact, nulliparous females exhibit hyperproliferation of mammary epithelial cells and increased mammary ductal branching (Gigliotti *et al*., 2003). Other phenotypes generated by the null mutation are improved performance in the contextual fear conditioning test of long-term memory (Sterneck *et al*., 1998) and further impairment of adipocytic differentiation *in vitro* caused by *Cebpb* gene deletion (Tanaka *et al*., 1997). In summary, Cebpd activity appears to play a role in proliferation, differentiation and apoptosis depending on the cell type and specific physiological response.

In this study we have characterized the effect of Cebpd deficiency in mouse embryonic fibroblasts (MEF). We found that lack of Cebpd results in genomic instability and centrosome amplifications *in vitro*. Furthermore, immortalized mutant MEF display several characteristics of transformation. Thus, we hypothesize that Cebpd is a potential candidate tumor suppressor gene based on its role in genome maintenance.

*Correspondence: E Sterneck; E-mail: sterneck@ncifcrf.gov
[3]Current address: Purdue Pharma LP, One Stamford Forum, Stamford, CT 06910, USA
Received 12 May 2003; revised 22 September 2003; accepted 16 October 2003

Results

Cebpd-*deficient fibroblasts exhibit impaired growth control*

MEF express *Cebpd* constitutively at low levels (data not shown). Freshly isolated MEF in culture grow rapidly at first, then cease to proliferate and senesce (crisis). Some cells escape senescence after a period of time and become established as cell lines. Figure 1 shows the growth curves of wild-type (WT) and *Cebpd*-deficient (KO) MEF from individual embryos using the classical 3T3 protocol (Todaro and Green, 1963). While the kinetics of establishment as a cell line varied significantly between different MEF isolates, we did not observe genotype-specific differences in growth rates before crisis or in the kinetics of crisis when averaging 10 WT MEF and seven KO MEF from five independent experiments (Figure 1, and data not shown). Furthermore, expression levels and kinetics of the $p16^{INK4a}$ gene, which is a marker of senescence (Palmero *et al*., 1997), were similar in KO and WT cells through the period of crisis (data not shown). However, within individual experiments, KO fibroblasts tended to recover more quickly from crisis either by shorter crisis period or more rapid acceleration of the growth rate thereafter (Figure 1). Therefore, lack of Cebpd does not affect the mechanisms involved in cell proliferation and induction of cellular senescence. However, subsequent to immortalization, lack of Cebpd promotes cell growth.

We next addressed the growth characteristics of immortalized MEF (3T3 MEF) in comparison with the NIH3T3 mouse fibroblast cell line and an NIH3T3 cell line transformed by the *Ki-ras* oncogene (Ras-NIH3T3; Janssen and Mier, 1997). Data obtained with two independently derived 3T3 MEF lines per genotype (KO-3T3: KO#1, KO#2; WT-3T3: WT#1, WT#2) demonstrated that *Cebpd*-deficient fibroblasts share many features characteristic of transformed cells. Titration of the serum concentration revealed that KO-3T3 were less sensitive to serum withdrawal than WT-3T3. When cultured at 0 or 0.07% serum, a significant proportion of WT-3T3 and NIH3T3 cells underwent apoptosis (Figure 2a). In contrast, KO-3T3 and Ras-NIH3T3 cells largely survived in the absence of serum, and at 0.07% serum even proliferated to some extent (Figure 2b). Apoptosis pathways *per se* are not defective in KO fibroblasts, since they responded normally to the apoptosis inducer tunicamycin (data not shown), indicating that the lower rate of cell death in KO cells in the absence of serum is specific to such culture conditions.

Normal adherent cell lines proliferate until confluent and then arrest in the G0 phase of the cell cycle. Accordingly, analysis of DNA content by flow cytometry showed that the G0/1 fraction of WT-3T3 and NIH3T3 cells was significantly increased in confluent cultures compared to exponentially growing cultures indicating cell cycle arrest (Figure 2c). In contrast, KO-3T3 did not display a significant shift of cells from the S + G2/M phases, representing proliferating cells, to the G0/1 population upon confluence. Ras-NIH3T3 cells were not included in this analysis because they grow in clumps and detach easily, which does not allow

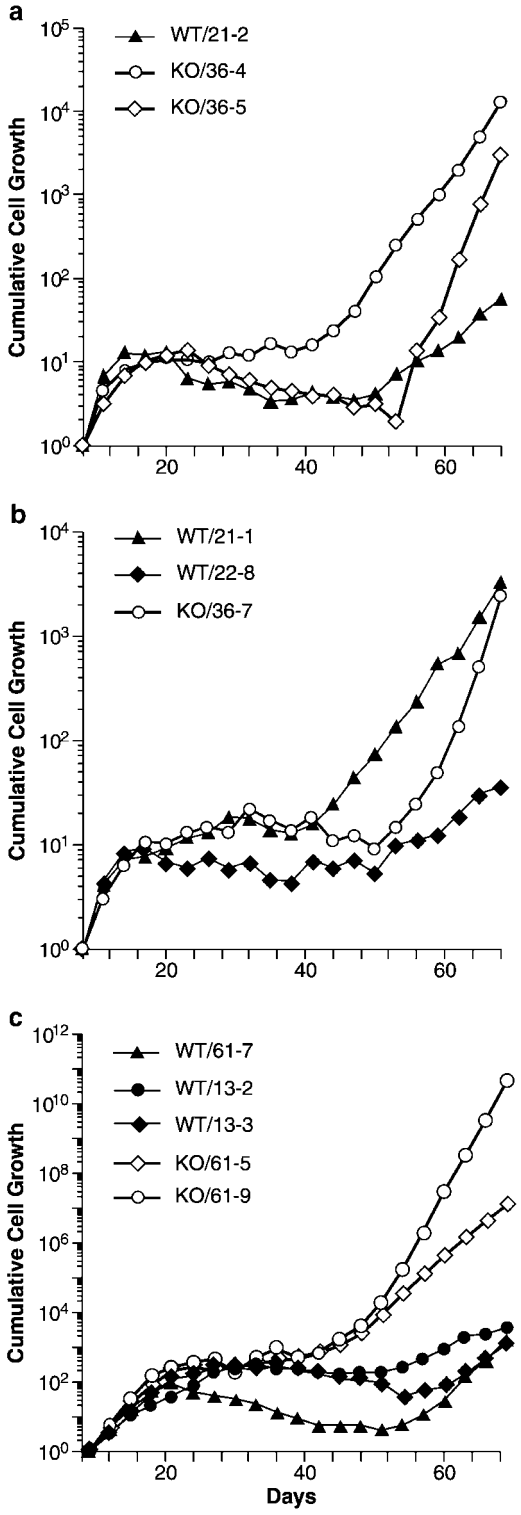

Figure 1 *Cebpd*-deficient MEF recover readily from crisis. Cumulative cell growth (3T3 protocol) of six WT and five KO primary MEF from individual embryos in three independent experiments (**a**–**c**) starting at passage three

determination of a confluent state. DAPI staining also showed that individual mitotic figures could still be found in KO-3T3 but not in WT-3T3 cultures that had been confluent for over 2 weeks (data not shown).

To further our analysis at the molecular level, we investigated expression of the growth arrest specific gene *Gas1*, which is induced by contact inhibition and serum withdrawal in NIH3T3 cells. Gas1 inhibits DNA synthesis and S-phase entry, and exhibits tumor suppressor activity in human tumor cell lines (Del Sal *et al*., 1992; Evdokiou and Cowled, 1998). Analysis of fibroblasts at confluence or in the absence of serum revealed that *Gas1* expression was inducible in both WT and KO cells (Figure 3a). However, mutant fibroblasts displayed significantly reduced levels of *Gas1* in all

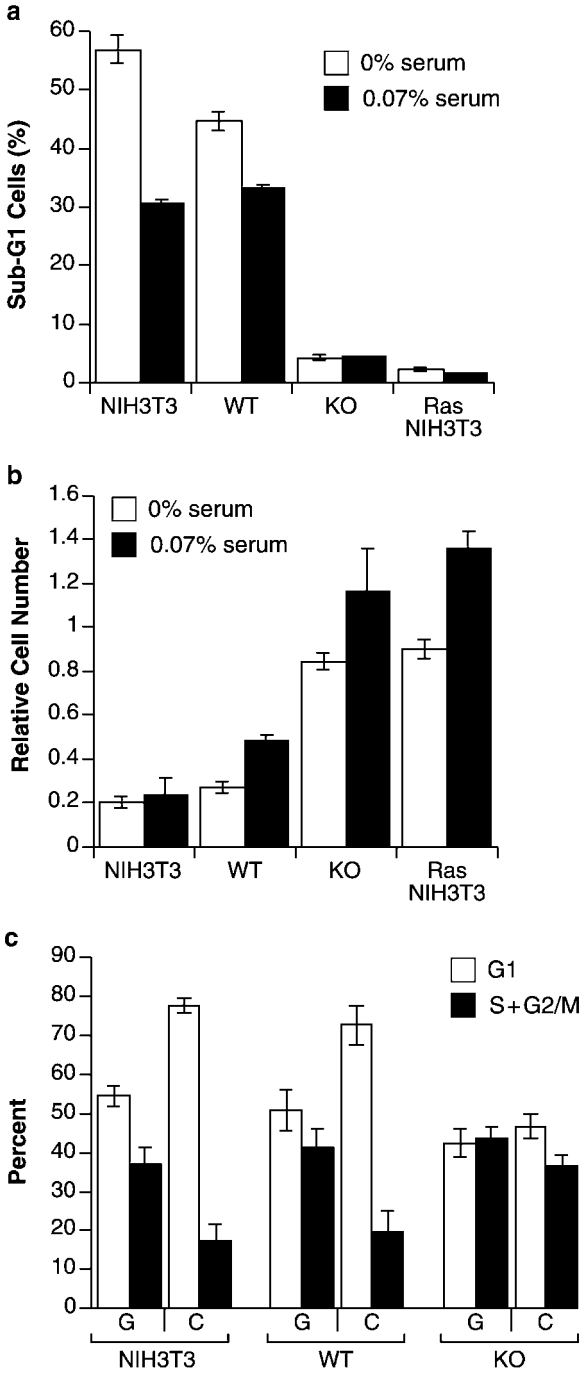

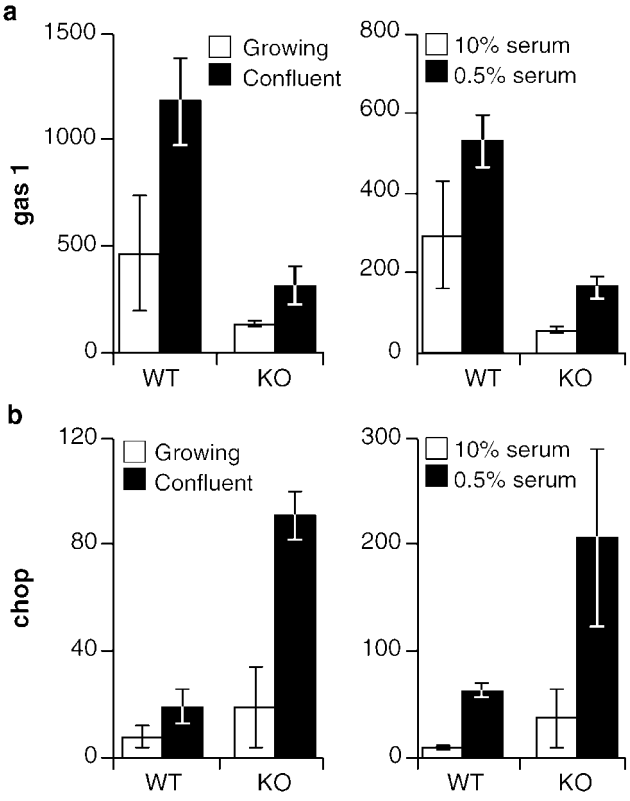

Figure 3 Altered gene expression response in *Cebpd* null 3T3 fibroblasts. Northern analysis of RNA from cells treated as described in Figure 2. The 10% serum group was harvested 2 days after seeding. 'WT' and 'KO' data represent the mean ± s.d. of the WT#1 and WT#2, and KO#1 and KO#2 lines, respectively. Expression levels of (**a**) *gas1* and (**b**) *Chop* were quantified by phosphoimage analysis, normalized against *cyclophilin* expression, and are expressed in arbitrary units

Figure 2 *Cebpd*-deficient 3T3 fibroblasts display reduced serum dependence and contact inhibition. 'WT' and 'KO' data represent the mean ± s.d. of the WT#1 and WT#2, and KO#1 and KO#2 lines, respectively. (**a**) Cell death upon serum withdrawal. Cells were seeded at 3×10^5 cells per 100 mm dish. The next day, the medium was changed to 0 or 0.07% serum. After 2 days, FACS analysis of the DNA content was performed. The sub-G1 populations are shown as a measure of cell death. Results represent the means and s.d. of duplicate experiments. (**b**) Cell survival upon serum withdrawal. Cells were seeded with 10% serum in 24-well plates at 2×10^4 cells per well. The following day, three wells were used to determine the cell number. For the remaining wells, the medium was changed to 0 or 0.07% serum following two washes with PBS. The number of cells per well was determined 48 h later. The data are expressed as relative cell survival (cell number at the time of serum reduction = 1). A representative experiment performed with triplicate wells for each cell line is shown. (**c**) Cell cycle distribution under subconfluent and confluent culture conditions. The cells were seeded at 3×10^5 cells per 100 mm dish, collected on day 2 (G, growing) or day 4 (C, confluent), and FACS analysis of the DNA content was performed to determine the cell cycle distribution (mean ± s.d. of % cells in G0/1 and S + G2/M of three independent experiments)

conditions suggesting that lower levels of *Gas1* are in part responsible for the impaired growth arrest response of KO-3T3 MEF. The blunted expression in KO cells is specific for *Gas1*, because expression of the Cebp-related gene *Chop* (also known as growth arrest and DNA damage (gadd) 153; Fornace *et al*., 1989) was instead upregulated in Cebpd-deficient cells (Figure 3b). Chop is present at low levels under normal conditions but is induced in response to various types of stress and can induce growth arrest acting around the G1/S checkpoint (Barone *et al*., 1994; Zinszner *et al*., 1998). Chop is required for cell death in response to stress mediated by the endoplasmic reticulum (ER) (Zinszner *et al*., 1998). In response to the ER stressor tunicamycin, *Chop* was induced to equivalent levels in WT- and KO-3T3 (data not shown), indicating that elevated levels of *Chop* in KO cells are specific to growth arrest conditions. Possibly, *Chop* is 'overinduced' in confluent and serum-starved KO fibroblasts due to a feedback regulatory mechanism that senses the impaired cellular response, but is not able to correct it. In summary, these data indicate that the rapid recovery of KO fibroblasts from crisis results from the acquisition of transformed features both at the molecular and cellular levels.

A frequent attribute of transformed cells is lack of anchorage dependence. When tested for the ability to form colonies in soft agar, only Ras-NIH3T3 cells were able to grow, but not KO or WT MEF (data not shown). However, on plastic dishes, KO MEF displayed rough colony edges similar to Ras-NIH3T3 cells (Figure 4). This phenotype is indicative of increased cell motility and reduced cell communication. WT MEF and NIH3T3 cells exhibited round colony edges. Given the number of transformed features of KO-3T3 MEF *in vitro*, we tested the tumorigenicity of immortalized MEF *in vivo*. Four out of four independent KO-3T3 lines formed tumors in nude mice. However, three out of four WT-3T3 lines were tumorigenic as well (data not shown). Tumorigenicity of WT MEF was surprising and is possibly due to the 129S1 mouse strain background used in this study. The time course and growth rate of the tumors varied significantly even within each cell line. Therefore, we could not identify a specific enhancement

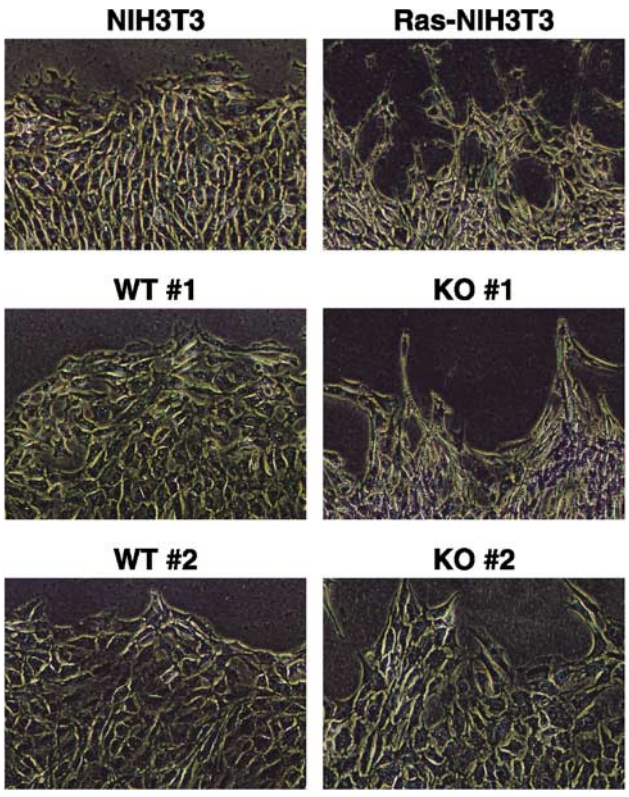

Figure 4 *Cebpd*-deficient 3T3 fibroblasts display rough colony edges. Photomicrographs of colony edges. The indicated cells were seeded at low density (500 cells per 10 cm dish), cultured for 10 days with medium changes every 3 days, and then stained with Giemsa ($\times$ 100 original magnification)

Table 1 Cebpd-deficient primary MEF display multiple chromosomal aberrations[a]

	Total		*WT*					*KO*			
	WT	*KO*	*#1*	*#2*	*#3*	*#4*	*#5*	*#1*	*#2*	*#3*	*#4*
Passage#			6	6	4	4	3	6	6	3	3
Ploidy ~2n	45	32	9	10	10	9	7	10	4	11	7
Ploidy ~3n	0	1	0	0	0	0	0	0	1	0	0
Ploidy ~4n	1	6	0	0	0	0	1	1	1	1	3
Ace	2	22	1	1	0	0	0	10	12	0	0
Chrb	3	1	0	0	0	1	2	1	0	0	0
Dic	1	25	0	1	0	0	0	11	14	0	0
Chtb	2	8	0	0	1	1	0	1	3	3	1
Rb	1	4	0	1	0	0	0	2	1	1	0
TR	0	2	0	0	0	0	0	0	2	0	0
Asyint	0	17	0	0	0	0	0	12	5	0	0
T	0	20	0	0	0	0	0	5	12	1	2
Del	0	17	0	0	0	0	0	3	11	0	3
Dp	0	6	0	0	0	0	0	1	0	1	4
CR	0	18	0	0	0	0	0	10	7	0	1

[a]Total number of metaphases analysed per isolate are grouped by ploidy of 2n, 3n and 4n. The number of structural aberrations identified by SKY analysis are listed: Ace (acentric fragments), Asyint (asymmetrical interchanges), Chrb (chromosome breaks), Chtb (chromatid breaks), CR (complex rearrangements), Del (deletions), Dic (dicentric chromosomes), Dp (duplications), Rb (Robertsonian translocations), T (translocations), TR (triradial, an exchange between two chromosomes, which results in a three armed configuration)

of *in vivo* tumorigenicity by the *Cebpd* mutation with this system.

Genomic instability in the absence of Cebpd

The transformed characteristics of KO-3T3 fibroblasts are not present prior to immortalization (data not shown) and therefore are not likely due to a direct role of Cebpd in these phenotypes. An indirect promotion of loss of growth control could result from a higher mutation rate or accumulation of chromosomal abnormalities in mutant cells. This hypothesis was suggested by the finding that KO cultures displayed giant lobular nuclei at low but consistent frequency indicating aneuploidy (data not shown, see also Table 1), and by reports that Cebpd can localize to centromeres during mitosis (Tang and Lane, 1999). Thus, we addressed increased genomic instability as a potential mechanism for acquisition of mutations in KO MEF.

Spectral karyotyping analysis (SKY) was performed on primary MEF at passages three to six in cultures isolated from four KO embryos and five WT embryos, and demonstrated that all four KO samples displayed a significant increase in nonhomologous rearrangements compared to WT MEF (Table 1; Figure 5). In summary, we identified 140 rearrangements involving chromatid or chromosome breaks in the four KO samples, compared to nine rearrangements in the five WT samples. The frequency of abnormal cells in the KO samples averaged from 18 to 77% and varied from a single chromosome break per cell to complex karyotypes like the one shown in Figure 5. Due to the complexity of cytogenetic aberrations, SKY did not allow us to evaluate net gain or loss of chromosomal material. However, analysis of gross changes in ploidy indicates a 10-fold increase in aneuploid cells in the KO cultures. The chromosomal abnormalities increased with passage number, suggesting that rearrangements accumulated over time (Table 1). In some cases more than two chromosomes were involved (Figure 5c). In particular, reciprocal translocations, deletions, duplications and complex rearrangements were observed in at least three of the four KO MEF, but not in any of the five WT MEF. However, no recurrent patterns were observed, indicating that no clonal outgrowth was taking place by passage six. To determine if the KO MEF contained an overall imbalance in DNA copy number, we analysed the different batches by comparative genomic hybridization (CGH). The results showed a normal profile for both WT and KO primary MEF (SKY and CGH results can be retrieved at http://www.ncbi.nlm.nih.gov/sky/skyweb.cgi), indicating that the chromosomal instability in KO MEF did not translate into the acquisition of clonal nonrandom chromosomal gains and losses detectable by CGH at passage six.

The degree of chromosomal rearrangements in primary KO MEF would suggest a higher rate of apoptosis in these cultures affecting cumulative growth. However, the growth rate of primary KO MEF was comparable to that of control MEF (Figure 1). To assess if accelerated growth, as seen with 3T3 KO MEF, was compensating for an elevated rate of apoptosis, we analysed the distribution of cells in the cell cycle and the fraction of apoptotic cells in up to 11 WT and eight KO primary MEF by FACS from day 5 to 22 in culture (passages 3–9). However, we found no difference between WT and KO cells (data not shown). Thus, despite the elevated level of chromosomal abnormalities, the KO MEF do not exhibit an increased rate of cell death. These data raise the possibility that lack of apoptosis in response to chromosomal abnormalities may be one mechanism by which KO cells accumulate damages.

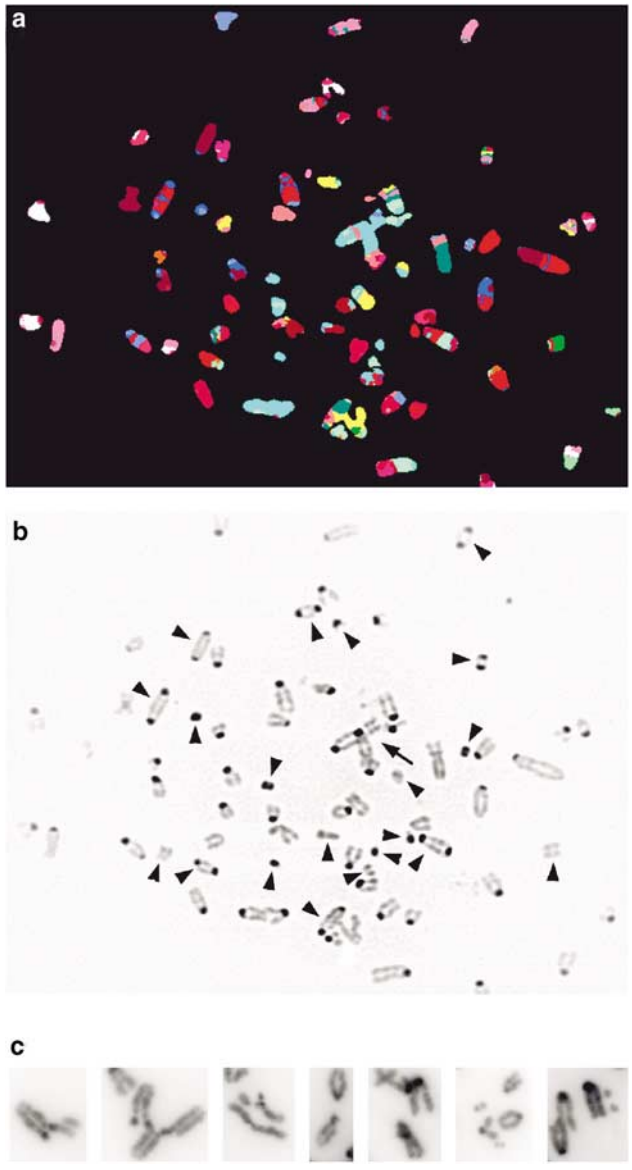

Figure 5 SKY analysis of primary MEF derived from *Cebpd*-deficient embryos. (**a**) Classification colors and (**b**) DAPI image for a metaphase from mutant MEF (KO#1 of Table 1) demonstrating significant chromosomal instability. The arrow indicates a complex rearrangement. Arrowheads point to acentric fragments, dicentric chromosomes and Robertsonian translocations. (**c**) Examples of rearrangements seen in different metaphases derived from KO#1 and KO#2 MEF (see Table 1)

Cellular architecture and genomic stability are controlled in part by centrosomes, the centers of microtubule array organization including mitotic spindles. Centrosome defects characterized by abnormal size and number have been implicated as a possible cause of mitotic abnormalities in tumor cells and loss of tissue architecture seen in solid tumors (Salisbury *et al*., 1999). Therefore we investigated a potential correlation between genomic instability and centrosome amplification. More than 100 interphase cells of two WT and two KO MEF isolates were stained with anti-γ-tubulin (Figure 6) or anti-centrin antibodies that allow centrosome identification in each stage of the cell cycle. Cells with more than two centrosomes were considered abnormal (Table 2). In WT MEF cultures, 6–14% of cells displayed abnormal centrosomes. The majority of the abnormal counts were three to four centrosomes. This could possibly be due in part to normal centriole duplications. However, centrosome amplifications were significantly more frequent in KO MEF and the centrosome numbers were more diverse. The total numbers of abnormal cells varied between anti-γ-tubulin and anti-centrin staining, possibly due to differences in cell passages or because of normal variations in the cells between experiments. In all, 27–51% of KO MEF cells exhibited centrosome amplifications, while at the gross level only 18% were aneuploid (as deduced from Table 1). These data suggest that defects in the centrosome cycle may precede ploidy changes and chromosomal rearrangements in *Cebpd* mutant cells.

In summary, the cytogenetic analyses demonstrate an increased level of centrosome amplification and genomic instability in primary *Cebpd* null MEF resulting in complex chromosomal rearrangements.

Discussion

Cancer is the result of multiple genetic changes, including activation of oncogenes and loss of normal function of tumor suppressor genes. Endogenous and environmental factors can lead to DNA damage driving

Table 2 Cebpd-deficient MEF display severe centrosome amplifications

	Centrosome number								
	Normal	*Abnormal*							
	1–2	*0*	*3*	*4*	*5*	*6*	*7*	*>7*	*%*
γ-Tubulin									
WT#1(P3)	143	0	6	11	1	3	0	3	14.3
WT#2(P3)	114	0	8	9	1	0	0	1	14.2
KO#1(P3)	78	2	10	16	2	2	2	8	35.0
KO#2(P3)	96	3	9	16	3	0	2	3	27.2
Centrin									
WT#1(P6)	139	0	4	8	0	1	0	0	8.5
WT#2(P5)	125	0	3	4	0	0	0	1	6.0
KO#1(P6)	65	5	15	22	3	5	3	15	51.1
KO#2(P8)	82	3	6	8	7	2	5	19	37.8

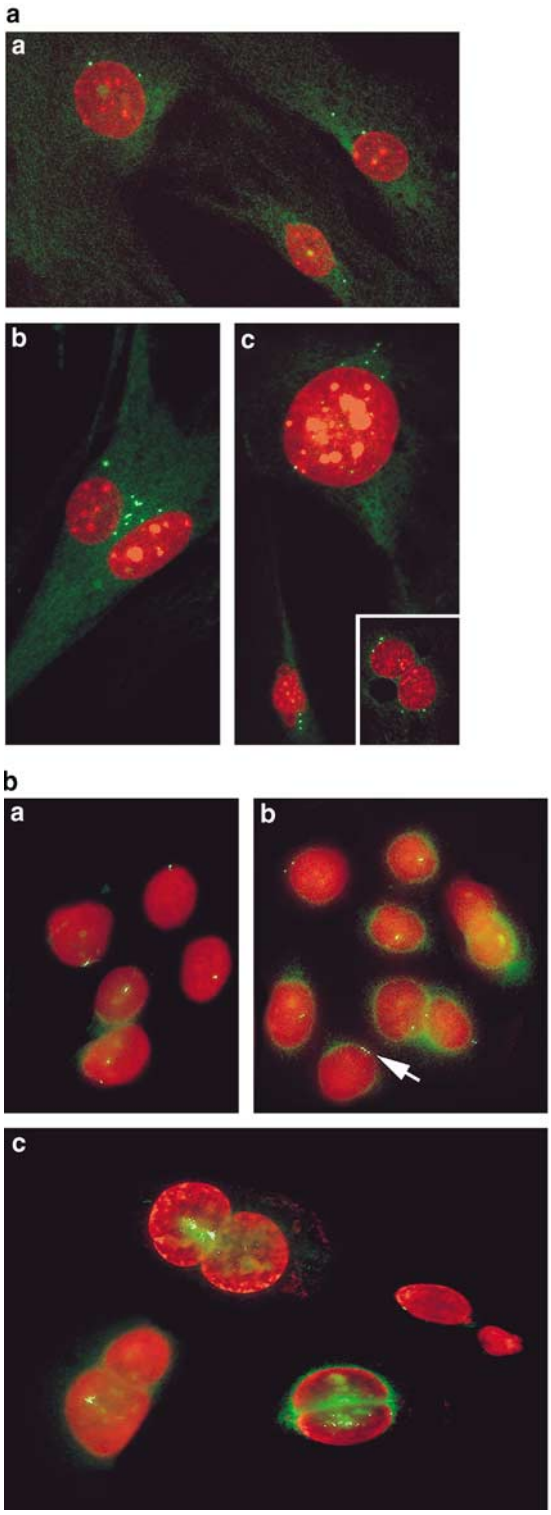

Figure 6 Centrosome duplications and aberrant arrangements in primary *Cebpd* null MEF. Immunocytochemistry with an antibody against (**a**) γ-tubulin and (**b**) centrin to detect centrosomes. (**a**a) Normal centrosomes in interphase nuclei; (**a**b) increased centrosome numbers grouped in the cytoplasm; (**a**c) detached centrosomes lined up, or as shown in the inset, distributed around the nucleus. (**b**a) Normal centrosomes in interphase nuclei; (**b**b) group of cells with normal centrosome numbers and one cell with one extra copy (arrowhead); (**b**c) cells with multiple centrosome copies grouped in the center of the cell

such mutations, and multiple mechanisms exist in the cell to repair the damage or to eliminate a cell beyond repair. Any perturbation of this balance such as genomic instability, which can be caused by many diverse mechanisms, will eventually lead to cancer (Hoeijmakers, 2001). We have found that *Cebpd* deficiency leads to chromosomal instability in primary MEF *in vitro* followed by loss of normal growth control. These data suggest that *Cebpd* could function as a tumor suppressor that acts on genome maintenance. As a transcription factor it may regulate the expression of genes that are essential for recombination and repair mechanisms or for cell cycle checkpoints and apoptosis in response to genome damage (Hoeijmakers, 2001). Differential expression analysis of primary WT and KO MEF could address this hypothesis. Alternatively, the physical association of Cebpd with the centromere (Tang and Lane, 1999) may affect centromere or kinetochore functions important for chromosome stability. Analysis of other known centromere-associated proteins and features may shed light on the functionality of this higher order chromatin organization in *Cebpd* null MEF. Considering the degree of genomic instability, it is unlikely that the aberrant growth regulation in established KO-3T3 fibroblasts is directly due to the absence of *Cebpd*. However, subsequent to immortalization, *Cebpd* deficiency may specifically cooperate with pathways that, for example, impair the expression of *Gas1*. CGH analysis of established lines should determine if certain recurrent genomic imbalances lead to clonal outgrowth of KO fibroblast lines.

A role for other *Cebp* genes in tumor development has already been demonstrated. Point mutations in the *CEBPA* gene that lead to truncated dominant negative proteins are associated with a subset of acute myeloid leukemia patients (Pabst *et al*., 2001). In mice, mammary epithelial cell specific overexpression of a dominant negative *Cebpb* transgene causes mammary tumors (Zahnow *et al*., 2001). On the other hand, *Cebpb*-deficient mice are completely resistant to chemical carcinogenesis of the skin. This phenotype may be due to an essential role of Cebpb in oncogenic Ras signaling (Zhu *et al*., 2002). These data suggest a potentially complex cell type and isoform specific modulation of normal and aberrant growth control by *Cebp* genes.

A potentially direct role for Cebpd in tumor suppressor pathways is suggested by the ability of Cebp proteins to associate with the hypophosphorylated form of the tumor suppressor retinoblastoma protein Rb1. In the case of Cebpb, this interaction facilitates DNA binding and promoter transactivation. The association of Rb1 with Cebpb is regulated since it occurs in cell lines specifically as they differentiate toward adipocytes or monocyte/macrophages (Chen *et al*., 1996a, b; Charles *et al*., 2001). The prominent Rb1-binding transcription factors of the E2f family have recently been shown to regulate a plethora of genes involved in DNA damage checkpoint and repair pathways, mitotic spindle checkpoints and chromosome segregation (Ren *et al*., 2002). Interestingly, the Cebpa protein can affect E2f association with different Rb family members (Timchenko *et al*., 1999), and can inhibit expression of E2f target genes (Slomiany *et al*., 2000; Johansen *et al*., 2001). Cebpa can also modulate protein levels of cdk2, cdk4 and cyclin A in part by nontranscriptional mechanisms (Wang *et al*., 2001; Welm *et al*., 2002; Wang *et al*., 2002). Furthermore, Cebp proteins including Cebpd have recently been shown to interact physically with Smad3 and Smad4 (Choy and Derynck, 2003). Smad proteins mediate signaling by the transforming growth factor, which can have oncogenic as well as tumor suppressor activity (Piek and Roberts, 2001) and has been implicated in the maintenance of genomic stability (Glick *et al*., 1999). In summary, these reports suggest a number of potential mechanisms by which Cebpd may affect chromosomal integrity.

In WT MEF we observed nine individual rearrangements in 46 metaphases and up to 14% of cells with abnormal centrosome numbers. These abnormalities are significant, yet substantially lower than those observed in the Cebpd-deficient MEF (140 rearrangements in 40 metaphases and up to 50% of cells with abnormal centrosome numbers). The study reported here is based on MEF derived from the 129S1 mouse strain. This strain was chosen because the *Cebpd* targeted mutation was generated in 129S1-derived embryonic stem cells, and therefore provides a genetically clean background for the comparison of WT and mutant MEF. When it was first observed that the EGF receptor KO had strain-specific consequences (Threadgill *et al*., 1995; Sibilia and Wagner, 1995), it became clear that mouse strains differ significantly and many similar reports have been published since. This phenomenon has led to the further elucidation of molecular pathways via identification of strain-specific modifier genes. Alternatively, systematic comparisons of WT strains also provide some insight into the regulation of basic physiological processes as well as the mechanisms leading to strain-specific mutant phenotypes. For example, the locus encoding p16INK4A and p19ARF harbors point mutations in the BALB/c mouse strain, which are responsible for the plasmacytoma susceptibility of this strain (Zhang *et al*., 1998; Zhang *et al*., 2001). Possibly, the 129S1 strain is genetically susceptible to centrosome duplications and genomic instability. Indeed, Cebpd deficiency may lead to genomic instability by cooperating with the specific molecular pathway that predisposes 129S1 cells to centrosome amplifications. Thus, it will be interesting to perform a comparison study of basal genomic stability and the effect of Cebpd deficiency in MEF from different mouse strains.

Genomic instability is often associated with centrosome amplifications. However, it is still unclear if centrosome alterations are a cause or consequence of genomic instability (Duensing and Munger, 2001). In some cases, multipolar spindles initiated by the supernumerary centrosomes, for example, as demonstrated in MEF with null mutations of *Tp53* (Fukasawa *et al*., 1996) or *Brca1* (Xu *et al*., 1999), can be correlated with genomic instability. However, we have previously observed that amplified centrosomes not always lead to multipolar spindles (Ghadimi *et al*., 2000). Thus, we

analysed primary WT and KO MEF with anti-α-tubulin antibodies. Despite the centrosome amplifications, we did not observe abnormal spindle structures in either genotype (data not shown). These data suggest that the amplified centrosomes are not functional and the chromosomal rearrangements may not be due to spindle aberrations. Rather, perturbation of one of the emerging additional functions of the centrosome in cell cycle progression and checkpoint control (Doxsey, 2001) may lead to genomic instability in Cebpd-deficient MEF.

Since KO MEF display genomic instability, why do we not observe spontaneous tumors in the KO mice or even developmental abnormalities? The transfer of cells to *in vitro* culture, as done with MEF in this study, releases them from growth control mechanisms and tissue-specific restrictions encountered *in vivo*. Presumably, this procedure can mimic the effect of advanced pro-oncogenic mutations. For example, mice with a null mutation of the cyclin-dependent kinase inhibitor p21/CIP1/WAF1 also develop normally, and the growth and senescence of null MEF *in vitro* is comparable to controls. However, the MEF display G1 checkpoint defects, and the mutation indeed contributes *in vivo* to tumorigenesis when induced by, for example, oncogenic Ras or chemical carcinogenesis (Deng *et al*., 1995; Pantoja and Serrano, 1999; Jackson *et al*., 2002). Since both Cebpa and Cebpb can affect p21 expression (Timchenko *et al*., 1996; Chinery *et al*., 1997), we addressed it in the Cebpd KO MEF but found p21 levels comparable to those in WT MEF.

Based on the KO MEF phenotype, we hypothesize that Cebpd may function as a tumor modifier in specific cell types, where it is highly expressed, and when challenged by induced mutagenesis via chemical mutagenesis or oncogenic transgenes. For example, lack of mismatch repair genes leads to tissue-specific tumors (Kreidberg and Natoli, 2001) although even MEF can display genomic instability, as shown for Msh2 (Reitmair *et al*., 1997). Expression of Cebpd is low to undetectable in most organs except lung and the involuting mammary gland (see Introduction). We are currently crossing the *Cebpd*-deficient mice to lung- and mammary-specific transgenic mouse tumor models to address the role of Cebpd as a tumor suppressor *in vivo*.

Materials and methods

Cell lines and mouse embryo fibroblasts

NIH3T3 (Jainchill *et al*., 1969) and Ras-NIH3T3 cells (Janssen and Mier, 1997) were maintained in Dulbecco's modified Eagle's medium (DMEM) supplemented with 10% fetal bovine serum (FBS), penicillin and streptomycin, unless indicated otherwise. MEF were isolated essentially as described (Tessarollo, 2001) from individual E13.5–E14.5 embryos generated by mating of *Cebpd* null heterozygous mice (Sterneck *et al*., 1998) of the 129S1 strain, and were frozen at passage two. The cells were maintained in DMEM/10% FBS and passaged every 3 days at 3×10^5 cells per 10 cm dish (3T3 protocol). The two established cell lines per genotype were derived from pooled KO and WT embryos of two independent litters each.

FACS analysis and cytological staining

For fluorescence-activated cell sorter analysis (FACS), cells were fixed with methanol (−20°C), treated with 100 μg/ml RNase A, stained with 50 μg/ml propidium iodide and analysed by flow cytometry using CellQuest software (Becton-Dickinson, CA, USA). For cytological staining, cells were cultured on Falcon chamber slides (Thomas Scientific, Swedesboro, NJ, USA) and fixed for 10 min with methanol (0°C). Incubation with a monoclonal anti-γ-tubulin antibody (Sigma, St Louis, MO, USA) or anti-centrin antibody (kindly provided by JL Salisbury) was performed overnight at 37°C and antibody complexes were detected with FITC-conjugated anti-mouse IgG (Sigma, St Louis, MO, USA) and counterstained with DAPI. For Giemsa staining, the colonies were fixed with methanol for 20 min at room temperature, stained with Giemsa (Life Technologies, Inc.) for 1 h, washed with water and air dried.

SKY/CGH

Metaphase chromosomes from five WT and four KO MEF at P3-6 were prepared following exposure to colcemid (2 h, final concentration 100 ng/ml) and standard hypotonic treatment followed by fixation in methanol/acetic acid. Spectral karyotyping was performed as described (Liyanage *et al*., 1996; Montagna *et al*., 2002). Chromosome aberrations were defined using the nomenclature rules from the International Committee on Standardized Genetic Nomenclature for Mice (Davisson, 1994). A total of 6–12 metaphases were analysed for each cell line. Gray level images were acquired using a CCD camera (CH250, Photometrics, Tucson, AZ, USA) mounted on a Leica DMRXA epifluorescence microscope, and pseudocolored using Leica Q-Fish software.

Genomic DNA from the five WT and four KO primary MEF isolates was extracted following standard procedures. DNA labeling, hybridization and detection were performed as described (Montagna *et al*., 2002). Images were acquired with a Leica DMRXA epifluorescence microscope (Leica, Wetzlar, Germany) using fluorochrome-specific filters (Chroma Technologies, Brattleboro, VT, USA). Quantitative fluorescence imaging and CGH analysis was performed using Leica CW4000CGH software (Leica Microsystem Imaging Solutions, Cambridge, UK). Further details for all Materials and methods can be found at http://www.riedlab.nci.nih.gov/.

RNA analysis

Total RNA was prepared by lysis of cells in Trizol reagent (Life Technologies, Inc.). The RNA was analysed by Northern blotting as described (Sterneck *et al*., 1997). Radiolabeled DNA probes were prepared from isolated cDNA clones for the indicated genes. The specific signals were quantified by phosphorimage analysis (Molecular Dynamics, ImageQuant™).

Acknowledgements
We thank Mary Beth Hilton, Barbara Shankle and Lori Warg for expert technical assistance, and Danny Wangsa for help with mouse SKY kits preparation. We thank David Ron, JL Salisbury, Claudio Schneider, Richard Janssen and Debbie Morrison for valuable reagents and advice; Karen Vousden's laboratory for generous support with resources and expert advice; Karen Vousden, Shyam Sharan and Lino Tessarollo for critical reading of the manuscript.

References

Barone MV, Crozat A, Tabaee A, Philipson L and Ron D. (1994). *Genes Dev.*, **8,** 453–464.

Billiard J, Grewal SS, Lukaesko L, Stork PJ and Rotwein P. (2001). *J. Biol. Chem.*, **276,** 31238–31246.

Breed DR, Margraf LR, Alcorn JL and Mendelson CR. (1997). *Endocrinology*, **138,** 5527–5534.

Cassel TN, Nordlund-Moller L, Andersson O, Gustafsson JA and Nord M. (2000). *Am. J. Respir. Cell Mol. Biol.*, **22,** 469–480.

Charles A, Tang X, Crouch E, Brody JS and Xiao ZX. (2001). *J. Cell. Biochem.*, **83,** 414–425.

Chen PL, Riley DJ, Chen Y and Lee WH. (1996a). *Genes Dev.*, **10,** 2794–2804.

Chen PL, Riley DJ, Chen-Kiang S and Lee WH. (1996b). *Proc. Natl. Acad. Sci. USA*, **93,** 465–469.

Chinery R, Brockman JA, Dransfield DT and Coffey RJ. (1997). *J. Biol. Chem.*, **272,** 30356–30361.

Choy L and Derynck R. (2003). *J. Biol. Chem.*, **278,** 9609–9619.

Davisson MT. (1994). *Gene*, **147,** 157–160.

Del Sal G, Ruaro ME, Philipson L and Schneider C. (1992). *Cell*, **70,** 595–607.

Deng C, Zhang P, Harper JW, Elledge SJ and Leder P. (1995). *Cell*, **82,** 675–684.

Doxsey S. (2001). *Nat. Rev. Mol. Cell Biol.*, **2,** 688–698.

Duensing S and Munger K. (2001). *Biochim. Biophys. Acta*, **1471,** M81–8.

Evdokiou A and Cowled PA. (1998). *Int. J. Cancer*, **75,** 568–577.

Fornace Jr AJ, Nebert DW, Hollander MC, Luethy JD, Papathanasiou M, Fargnoli J and Holbrook NJ. (1989). *Mol. Cell. Biol.*, **9,** 4196–4203.

Fukasawa K, Choi T, Kuriyama R, Rulong S and Vande Woude GF. (1996). *Science*, **271,** 1744–1747.

Ghadimi BM, Sackett DL, Difilippantonio MJ, Schrock E, Neumann T, Jauho A, Auer G and Ried T. (2000). *Genes Chromosomes Cancer*, **27,** 183–190.

Gigliotti AP and DeWille JW. (1998). *J. Cell. Physiol.*, **174,** 232–239.

Gigliotti AP and DeWille JW. (1999). *Breast Cancer Res. Treat.*, **58,** 57–63.

Gigliotti AP, Johnson PF, Sterneck E and DeWille JW. (2003). *Exp. Biol. Med. (Maywood)*, **228,** 278–285.

Glick A, Popescu N, Alexander V, Ueno H, Bottinger E and Yuspa SH. (1999). *Proc. Natl. Acad. Sci. USA*, **96,** 14949–14954.

Hoeijmakers JH. (2001). *Nature*, **411,** 366–374.

Jackson RJ, Adnane J, Coppola D, Cantor A, Sebti SM and Pledger WJ. (2002). *Oncogene*, **21,** 8486–8497.

Jainchill JL, Aaronson SA and Todaro GJ. (1969). *J. Virol.*, **4,** 549–553.

Janssen RA and Mier JW. (1997). *Mol. Biol. Cell*, **8,** 897–908.

Johansen LM, Iwama A, Lodie TA, Sasaki K, Felsher DW, Golub TR and Tenen DG. (2001). *Mol. Cell. Biol.*, **21,** 3789–3806.

Kreidberg JA and Natoli TA. (2001). *Tumor Suppressor Genes in Human Cancer*, Fisher DE (ed). Humana Press Inc.: Totowa, NH, pp. 3–28.

Liyanage M, Coleman A, du Manoir S, Veldman T, McCormack S, Dickson RB, Barlow C, Wynshaw-Boris A, Janz S, Wienberg J, Ferguson-Smith MA, Schrock E and Ried T. (1996). *Nat. Genet.*, **14,** 312–315.

Montagna C, Andrechek ER, Padilla-Nash H, Muller WJ and Ried T. (2002). *Oncogene*, **21,** 890–898.

O'Rourke JP, Newbound GC, Hutt JA and DeWille J. (1999). *J. Biol. Chem.*, **274,** 16582–16589.

Pabst T, Mueller BU, Zhang P, Radomska HS, Narravula S, Schnittger S, Behre G, Hiddemann W and Tenen DG. (2001). *Nat. Genet.*, **27,** 263–270.

Palmero I, McConnell B, Parry D, Brookes S, Hara E, Bates S, Jat P and Peters G. (1997). *Oncogene*, **15,** 495–503.

Pantoja C and Serrano M. (1999). *Oncogene*, **18,** 4974–4982.

Piek E and Roberts AB. (2001). *Adv. Cancer Res.*, **83,** 1–54.

Ramji DP and Foka P. (2002). *Biochem. J.*, **365,** 561–575.

Reitmair AH, Risley R, Bristow RG, Wilson T, Ganesh A, Jang A, Peacock J, Benchimol S, Hill RP, Mak TW, Fishel R and Meuth M. (1997). *Cancer Res.*, **57,** 3765–3771.

Ren B, Cam H, Takahashi Y, Volkert T, Terragni J, Young RA and Dynlacht BD. (2002). *Genes Dev.*, **16,** 245–256.

Salisbury JL, Whitehead CM, Lingle WL and Barrett SL. (1999). *Biol. Cell*, **91,** 451–460.

Sibilia M and Wagner EF. (1995). *Science*, **269,** 234–238.

Slomiany BA, D'Arigo KL, Kelly MM and Kurtz DT. (2000). *Mol. Cell. Biol.*, **20,** 5986–5997.

Sterneck E, Paylor R, Jackson-Lewis V, Libbey M, Przedborski S, Tessarollo L, Crawley JN and Johnson PF. (1998). *Proc. Natl. Acad. Sci. USA*, **95,** 10908–10913.

Sterneck E, Tessarollo L and Johnson PF. (1997). *Genes Dev.*, **11,** 2153–2162.

Sugahara K, Sadohara T, Sugita M, Iyama K and Takiguchi M. (1999). *Cell Tissue Res.*, **297,** 261–270.

Takiguchi M. (1998). *Int. J. Exp. Pathol.*, **79,** 369–391.

Tanaka T, Yoshida N, Kishimoto T and Akira S. (1997). *EMBO J.*, **16,** 7432–7443.

Tang QQ and Lane MD. (1999). *Genes Dev.*, **13,** 2231–2241.

Tessarollo L. (2001). *Methods Mol. Biol.*, **158,** 47–63.

Threadgill DW, Dlugosz AA, Hansen LA, Tennenbaum T, Lichti U, Yee D, LaMantia C, Mourton T, Herrup K, Harris RC, Barnard YA, Yuspa SH, Coffey RY and Magnuson T. (1995). *Science*, **269,** 230–234.

Timchenko NA, Wilde M, Iakova P, Albrecht JH and Darlington GJ. (1999). *Nucleic Acids Res.*, **27,** 3621–3630.

Timchenko NA, Wilde M, Nakanishi M, Smith JR and Darlington GJ. (1996). *Genes Dev.*, **10,** 804–815.

Todaro G and Green H. (1963). *J. Cell Biol.*, **17,** 299–313.

Umayahara Y, Ji C, Centrella M, Rotwein P and McCarthy TL. (1997). *J. Biol. Chem.*, **272,** 31793–31800.

Wang H, Goode T, Iakova P, Albrecht JH and Timchenko NA. (2002). *EMBO J.*, **21,** 930–941.

Wang H, Iakova P, Wilde M, Welm A, Goode T, Roesler WJ and Timchenko NA. (2001). *Mol. Cell*, **8,** 817–828.

Welm AL, Timchenko NA, Ono Y, Sorimachi H, Radomska HS, Tenen DG, Lekstrom-Himes J and Darlington GJ. (2002). *J. Biol. Chem.*, **277,** 33848–33856.

Xu X, Weaver Z, Linke SP, Li C, Gotay J, Wang XW, Harris CC, Ried T and Deng CX. (1999). *Mol. Cell*, **3,** 389–395.

Zahnow CA, Cardiff RD, Laucirica R, Medina D and Rosen JM. (2001). *Cancer Res.*, **61,** 261–269.

Zhang S, Ramsay ES and Mock BA. (1998). *Proc. Natl. Acad. Sci. USA*, **95,** 2429–2434.

Zhang SL, DuBois W, Ramsay ES, Bliskovski V, Morse III HC, Taddesse-Heath L, Vass WC, DePinho RA and Mock BA. (2001). *Mol. Cell. Biol.*, **21,** 310–318.

Zhu S, Yoon K, Sterneck E, Johnson PF and Smart RC. (2002). *Proc. Natl. Acad. Sci. USA*, **99,** 207–212.

Zinszner H, Kuroda M, Wang X, Batchvarova N, Lightfoot RT, Remotti H, Stevens JL and Ron D. (1998). *Genes Dev.*, **12,** 982–995.